



**HAL**  
open science

## Towards the improvement of the ONERA transonic S3Ch wind tunnel

Brion Vincent, Julien Dandois, Marie Couliou, Daniel Florentin

► **To cite this version:**

Brion Vincent, Julien Dandois, Marie Couliou, Daniel Florentin. Towards the improvement of the ONERA transonic S3Ch wind tunnel. STO-AVT-338 - Specialists' Meeting on 'Advanced Wind Tunnel Boundary Simulation', May 2021, Berlin, Germany. hal-03255343

**HAL Id: hal-03255343**

**<https://hal.science/hal-03255343>**

Submitted on 9 Jun 2021

**HAL** is a multi-disciplinary open access archive for the deposit and dissemination of scientific research documents, whether they are published or not. The documents may come from teaching and research institutions in France or abroad, or from public or private research centers.

L'archive ouverte pluridisciplinaire **HAL**, est destinée au dépôt et à la diffusion de documents scientifiques de niveau recherche, publiés ou non, émanant des établissements d'enseignement et de recherche français ou étrangers, des laboratoires publics ou privés.

# Towards the improvement of the ONERA transonic S3Ch wind tunnel

**Brion Vincent**

Dandois Julien

Couliou Marie

Florentin Daniel

ONERA, 8 rue des Vertugadins, 92190 Meudon  
FRANCE

[vincent.brion@onera.fr](mailto:vincent.brion@onera.fr)

**Keywords:** Specialist Meeting, wind tunnel, numerical simulation, measurements

## ***ABSTRACT***

*Modern CFD techniques offer new opportunities to upgrade wind tunnels. Here we apply a RANS model to compute the flow through the circuit of the S3Ch transonic wind tunnel of ONERA Meudon center. The flow is set by implementing a disc of actuation at the location of the fan and total pressure and temperature losses at the location of the heat exchanger in the settling chamber. The methodology is validated against a reduced set of experimental flow data available in the settling chamber and test section. The results are considered along with standard design guidelines to define modifications to this circuit in order to improve flow quality. The new circuit will be implemented when the wind tunnel is moved to a different location in the near future. Another part of the work is dedicated to the calculation of the adaptive top and bottom walls of the test section. As an attempt to upgrade the current tool which uses a linearized potential model of the flow inside the test section, we consider a RANS approach and define a new optimization process to minimize the impact of the walls on the flow of interest compared to the flow in free flight conditions. The new methodology is applied to the particular case of a wing airfoil in transonic conditions and shows close to perfect correction when considering simulated data alone.*

## **1.0 INTRODUCTION**

The ONERA transonic S3Ch wind tunnel is a mid-scale facility that was built in 1948 to serve as a 1/8<sup>th</sup> scale prototype of the S1MA large scale wind tunnel in ONERA Modane (in the Alps), that was under construction at the time. The S3Ch wind tunnel underwent a profound upgrade in 1987 which led to the loss of similarity with the S1MA wind tunnel. The wind tunnel was equipped with a novel heat exchanger installed at the upstream end of the settling chamber, but also with adaptive upper and lower walls and a new convergent nozzle. Half of the circuit from the test section (included) to the downstream end of the propeller was redesigned to provide pressurization capabilities and the engine of the propeller was changed accordingly to reach a maximum power of 3.5MW. The overall pressurization of the tunnel was not completed though and the contemporary design of the wind tunnel is limited to operating at atmospheric conditions. A large part of the operation of the wind tunnel was also automated such that the modernized wind tunnel could be handled by a reduced set of persons. This already long story will continue soon when the S3Ch wind tunnel moves to ONERA headquarter in Palaiseau (Paris area). The move is programmed in 2025. This creates the opportunity to modify the tunnel circuit and its utilities for improvements. We discuss this matter in this paper.

Specifically we present the numerical simulation activities that have been conducted in the past few years to provide inputs and help define a new design for the tunnel circuit. The organisation of the paper is as follows. A description of the wind tunnel and its components is given in section 2. A particular attention is paid to the adaptive wall system. The numerical setup for the flow simulation, the results and experimental comparisons are then provided in section 3. Section 4 presents a preliminary evaluation of a CFD based technique to calculate the shape of the adaptive walls. We conclude in section 5.

## Overview of the recent simulations and experimental works dedicated to the improvement of the ONERA transonic S3Ch wind tunnel

### 2.0 THE ONERA S3CH TRANSONIC TUNNEL

#### 2.1 Description

The S3Ch features a rectangular test section of width 0.804m, height 0.764m and length 2.2m. This yields a Reynolds number  $Re_{ts}$  in the range  $1-10 \times 10^6$  ( $Re_{ts}$  is based on the equivalent test section diameter  $D_{ts} = S_{ts}^{1/2}$  with  $S_{ts}$  the cross section area of the test section) and a Mach number  $M_{ts}$  in the range 0.2-1.3. The supersonic regime is attained by shaping the upper and lower walls of the wind tunnel, which are adaptable (see the dedicated section below) into a first throat upstream and divergence downstream. The wind tunnel is equipped with a second throat downstream of the test section to stabilize the flow in the high subsonic regime (typically above Mach equal to 0.7). The circuit is 24m long and 5m wide (distances from circuit axis). The turbulence level of the wind tunnel in the transonic regime is given in terms of  $N$  factor and is equal to approximately 5.5 [1]. A diagram of the wind tunnel is shown in Figure 1. The different components and their characteristics are described in Table 1.

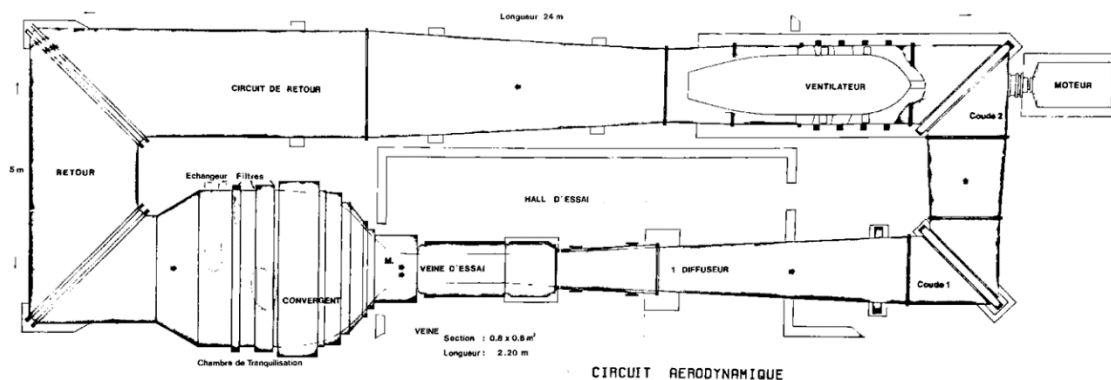


Figure 1: Diagram of the current circuit of the ONERA S3Ch transonic wind tunnel.

The wind tunnel allows a wide range of measurements techniques. On top of traditional measurements (pressure, temperature, humidity), Schlieren visualisations, probe apparatus and force sensors, most modern optical measurement techniques are employed: Particle Image Velocimetry (PIV), Laser Doppler Velocimetry (LDV), Pressure and Temperature Sensitive Paint (steady and unsteady PSP and TSP), Model Deformation Measurements (MDM).

Table 1: Components of the S3Ch wind tunnel and their properties

Components	Characteristics
Test section	Size $w_{ts} = 0.804\text{m}$ , $h_{ts} = 0.764\text{m}$ , $l_{ts} = 2.2\text{m}$
2 <sup>nd</sup> throat	Variable width from 0.55 to 0.87m
1 <sup>st</sup> diffuser	Circular section, cone angle = $5.5^\circ$ , length 6m
1 <sup>st</sup> & 2 <sup>nd</sup> corners	9 Vanes with thick profiles Diameter 1 <sup>st</sup> corner 1.875m, 2 <sup>nd</sup> corner 2.1m
Recovery grids	1 <sup>st</sup> grid : wire 6mm, cells 33.5mm, porosity 77%

### Overview of the recent simulations and experimental works dedicated to the improvement of the ONERA transonic S3Ch wind tunnel

	2 <sup>nd</sup> grid : wire 1mm, cells 5.5mm, porosity 67%
<b>Fan</b>	Two stage 24 blades each, propelled by an electric engine of 3.5MW, constant rotational speed 1500rpm
<b>2<sup>nd</sup> diffuser</b>	Circular section, cone angle = 7°, length 6.4m
	diameter 2.91m
<b>3<sup>rd</sup> &amp; 4<sup>th</sup> corners</b>	20 vanes made of curved plates Separation between vanes $s = 185\text{mm}$
<b>Rapid diffuser</b>	Circular to square, cone angle = 23°, length 2.2m Presence of cone trunks to drive the flow
<b>Settling chamber</b>	Size $w_{sc} = 4.2\text{m}$ , $h_{sc} = 4.2\text{m}$ , $l_{sc} = 3\text{m}$ Valves for equilibrium with Atmospheric pressure
<b>Heat Exchanger</b>	Power 2.5MW
	Hexagonal cells of width $w_h = 10\text{mm}$
<b>Honeycomb</b>	length $l_h = 155\text{mm}$ ratio $l_h/w_h = 15.5$
	Identical, at a distance 0.5m from honeycomb
<b>Turbulent grid 1 &amp; 2</b>	Wire diameter $d_{tg} = 0.5\text{mm}$ , cell $w_{tg} = 1.5\text{mm}$ porosity 44% separation between grids = 0.4m ( $0.1h_{sc}$ )
<b>Convergent Nozzle</b>	Area ratio inlet / outlet = 29.1

Due to its mid-scale range, the S3Ch wind tunnel is ideal for investigating elementary aerodynamic problems with the goal of exploring new flow phenomena, improving physical understanding and delivering accurate databases for the validation of flow solvers. The field of applications of the wind tunnel is wide, encompassing both external, internal aerodynamics and fluid structure interactions for applications such as airfoil and wing aerodynamics (generally in half wing configurations), small scale aircraft models, jets, jet engine / wing configurations, air intakes, launchers, rockets, etc. The wind tunnel also serves to investigate fundamental flows such as jet and wake dynamics, shock dynamics (e.g. buffet [2]), laminar to turbulent transition and new methods for flow control (shock dynamics, jet mixing, fluid structure interactions [3]).

Several facilities in the same range as the S3Ch wind tunnel exist in Europe that we list in Table 2, with their main information. Beware that the range of Mach number is essentially indicative as it takes the minimum and maximum possible values without consideration of the specific operational constraints. The size of the test section is given in terms of the diameter  $D_t$ , defined earlier. Table 2 does not list the European large scale transonic facilities, namely the ONERA S1MA and S2MA in France, the ARA transonic wind tunnel (TWT) in UK and the European Transonic Wind tunnel (ETW) in Germany, as they belong to an upper range of facilities. We do not talk either to the many other transonic facilities that exist throughout the world.

**Table 2: Selection of European transonic mid-scale wind tunnels**

Wind Tunnel	Type	Total Pressure (bar)	Max Reynolds (x $10^6$ )	Mach range	Test section size $S^{1/2}$ (m)
<b>TWG (DNW)</b>	Continuous	0.3-1.5	1.8	0.3-2.2	1.4
<b>PT1 (CIRA)</b>	Continuous	1.05-1.8	12-27	0.1-1.4	0.57
<b>S3Ch (ONERA)</b>	Continuous	1	3	0.1-1.4	1.1
<b>TST-27 (TU Delft)</b>	Blow down	2.5-20	38-130	0.5-4.2	0.39
<b>TWM (UNIBW)</b>	Blow down	1.2-5.0	10-80	0.3-3	0.74

## Overview of the recent simulations and experimental works dedicated to the improvement of the ONERA transonic S3Ch wind tunnel

<b>T1500 (FFA) [4]</b>	Continuous	1-5.5	1-10	0.3-1.2	2.12
------------------------	------------	-------	------	---------	------

### 2.2 Adaptive walls apparatus

S3Ch wind tunnel is equipped with adaptive upper and lower walls in order to reduce wall interferences. The principle is best understood for a two-dimensional flow, in which case the objective is to shape the walls into the streamlines that the flow would have if it was under free flight conditions. For a general three-dimensional flow, the shape results from an optimization process targeting minimized flow perturbations by the walls in the region around the model, as is described further below. The possibility to adjust the shape of the walls reduces the risk of flow blockage that becomes particularly strong in transonic conditions and further allows adjusting the incidence of the upstream flow to create effective angle of attack effects. The decisive advantage of such adaptive plain walls compared to traditional perforated or slotted walls is that the boundary conditions at these walls are more easily handled by numerical solvers. A full description of the S3Ch adaptive walls is provided in Le Sant and Bouvier [5]. We provide below the main information to understand how it works.

The technology was designed after the last upgrade of the wind tunnel in the early 90'. The hardware of the flexible wall is made as follows. The walls at flow side are made of 3mm thick duralumin plates of length 2.2m. The elastic deformations of these plates are performed in the vertical direction by 15 mechanical jacks homogeneously distributed along the overall plate length and driven by electric stepper motors. Each jack is capable of a 50mm displacement up or down, yet any part of the plate is constrained to a maximum 3° deformation angle. The flow information at each wall is obtained by a set of 400 pressure taps distributed along 4 longitudinal lines placed at each quarter width in span. The complete mechanism provides a two-dimensional correction to the flow.

The shape of the wall is calculated using an optimization approach that takes into account a description of the flow with the linearized potential flow theory. The flow is described by a three-dimensional potential which is a solution of the Laplace equation  $\Delta\beta\phi=0$  where  $\Delta\beta=\beta^2\partial_{xx}+\partial_{yy}+\partial_{zz}$  and  $\beta=(1-M^2)^{1/2}$  with  $M$  the Mach number. Using the linearity of the flow model, the flow in the test section is usefully decomposed into the following components

$$\phi = \phi^m + \phi^s + \phi^d \quad (1)$$

where  $\phi^m$  is the potential associated with the model,  $\phi^s$  that associated with the side walls and  $\phi^d$  that associated with the upper and lowers flexible walls. The  $\phi^s$  component can be calculated as the image effect of the model about the side walls so it is known once the model representation  $\phi^m$  is determined following

$$\phi^s(x,y,z)=\sum_{k=0..\infty}\phi^m(x,y+2kw_{ts},z) \quad (2)$$

The latter is made of elementary three-dimensional singularities (sources, doublets and horseshoe vortices) manually distributed in the region of the model. Their intensities are adjusted by matching the pressure distribution at the upper and lower walls when these walls are flat. Indeed in this case, the upper and lower wall representation  $\phi^d$  can be also calculated using the image effect. Furthermore a crosswise decomposition into Fourier components can also be introduced due to the periodicity effect of the lateral walls

$$\phi^d(x,y,z)=\sum_{k=0..\infty}\phi_n^d \cos(n\pi y) \quad (3)$$

---

## Overview of the recent simulations and experimental works dedicated to the improvement of the ONERA transonic S3Ch wind tunnel

The component  $n=0$  represents the two-dimensional cross-wise component.

The wall pressure is transformed into the vertical perturbation velocity component at the wall by using the Bernoulli relation. A least square algorithm is then used to evaluate the required intensities of the singularities (which are in fewer numbers compared to the pressure taps). Note that in practice the walls need not be flat to measure the wall pressure and calculate  $\phi^m$  by matching since the pressure can be corrected to that of a flat wall by an analytical relation deduced from the general solution of  $\phi^d$  (not detailed here).

Once the model representation  $\phi^m$  is available, the pressure distribution at the walls is used to calculate  $\phi^d$  and the complete wall interference component  $\phi^w = \phi^s + \phi^d$  is obtained. The process requires a constant to be determined as a consequence of the too numerous boundary conditions available for the potential  $\phi^d$ . This constant is set by matching the Mach inferred from  $\phi^d$  and the Mach number measured at some location inside the test section outside of the model effect (typically near the entrance of the test section). In a last step, a specific zone of interest in the flow is chosen (typically where the model is) where the effect of wall interferences is to be minimized. Minimization is then carried out by inverting the matrix representing the sensitivity of the flow field in this region of interest due to the deformation of the upper and lower walls.

It is important to keep in mind that the interferences are three-dimensional and that the adaptive walls only correct for the two-dimensional component (in terms of the span wise Fourier decomposition of the flow). The correct setting of the position, number and types of singularities representing the model requires some know-how by the wind tunnel operator.

The adaptive wall method is very powerful to correct the flow in the S3Ch wind tunnel for any kind of experimental test. The method handles all possible situations even in the cases when only one of the adaptive walls (either the upper or the lower one) is used (this is often done to allow for a window access for measurements, which requires a flat wall). In such a situation, image effects are used to mirror the one adaptive wall available and the corrected flow is that of the model and its image. Eventually the method allows defining a corrected Mach number  $Mc$  which is an approximate value of the Mach number of the model in free flight, that is, only due to  $\phi^m$ . This corrected Mach number is generally used as a first guess to set a numerical simulation free of the wind tunnel walls when the objective is to compute the experimental test case. The Mach number for the simulation is then refined to mimic the experimental results (sometimes also the flow incidence or other test parameters of interest are varied for perfect match).

The computational time of the method is negligible which allows its use in real time to correct the flow directly when operating the wind tunnel. In practice, wall adaptation is performed at every new setting of the flow parameters, for instance Mach number or angle of attack.

The power of the method holds in linearity of the flow model. In most situations, the hypothesis is valid because the model size is small enough compared to the test section and thus the effect of the model at the wall remains small. Note that this also means that a precise representation of the model is not required, which is why a reduced set of singularities distributed in the model area are very effective to provide the right wall deformation.

There are however legitimate questions on the validity of the approach in several situations, namely when strong shock waves are present or when the model effect is too large for the linearity hypothesis to hold (cases of large models, or large incidences for instance). Besides, the code being completely specific, there is a problem of maintenance. That is why we are currently considering upgrading the adaptive wall computational method to a more versatile, more easily maintained, CFD based tool. We show development in that sense in section 4, which should be considered as a feasibility and first trial analysis.

---

## Overview of the recent simulations and experimental works dedicated to the improvement of the ONERA transonic S3Ch wind tunnel

### 3.0 NUMERICAL SIMULATION OF THE TUNNEL CIRCUIT

#### 3.1 Methodology for the simulations

Numerical simulations of the circuit have been performed to explore new designs. These simulations use a Reynolds Averaged Navier-Stokes (RANS) description for the mean flow in the three-dimensional domain bounded by the wind tunnel circuit. The RANS model uses the Spalart-Allmaras turbulence closure. We use the elsA software [6] for these simulations.

The domain is meshed using a hybrid technique based on the CAD (Computer Aided Design) description of the wind tunnel. This design is the theoretical design obtained from the original paper drawings of the wind tunnel. It is important to mention that it may differ from the real geometry and that this may affect the numerical / experimental agreement. The four corners of the wind tunnel as well as the rapid diffuser are meshed with an unstructured grid and the linear parts are meshed with a structured grid. The total mesh has a cell count of approximately 265 Million. Boundary layers at the wall of the circuit and vanes are refined following usual practice ( $y^+ = 1$ ). Note that some of the wind tunnel components are not considered in the mesh: honeycomb and grids, fan and the heat exchanger. Due to the complexity of the mesh, no mesh convergence analysis has been performed.

The numerical problem is completed with an adiabatic wall boundary condition at the walls of the circuit and vanes. The pressure jump at the fan is modelled using an actuator disc condition and the heat exchanger in the settling chamber is reproduced by a “heat exchanger” type of boundary condition recently implemented in elsA, which allows to prescribe a pressure and temperature loss as a function of the mass flow rate. The mass flow rate is considered for an operating point Mach equal to 0.7 in the test section. In this case the pressure loss is set equal to 1000Pa, which encompasses the combined effect of the heat exchanger, the honeycomb and the two turbulent grids placed further downstream in the settling chamber. The value of the pressure jump at the fan serves as a numerical degree of freedom to adjust the Mach number in the test section to the desired value. The temperature loss is determined according to the power of the heat exchanger.

#### 3.1 Application to the current circuit

The numerical simulation is realized for a Mach number equal to 0.7 in the test section. The pressure jump imposed at the fan location in the numerical simulation to reach this Mach number matches the experimental value (6800 Pa) which validates the computational settings in terms of pressure loss in the circuit. Figure 1 (a) shows the Mach number field and the pseudo-streamlines in a horizontal slice of the circuit. The coordinate system ( $X_c, Y_c, Z_c$ ) is used for the circuit. Figure 1 (b) shows the field of total pressure. The term pseudo-streamline refers to the lines parallel to the flow field in that plane, which does not take into account the out of plane component. The maximum Mach number is reached in the test section. The flow slows down continuously up to the settling chamber and regains speed in the nozzle upstream of the test section.

**Overview of the recent simulations and experimental works dedicated to the improvement of the ONERA transonic S3Ch wind tunnel**

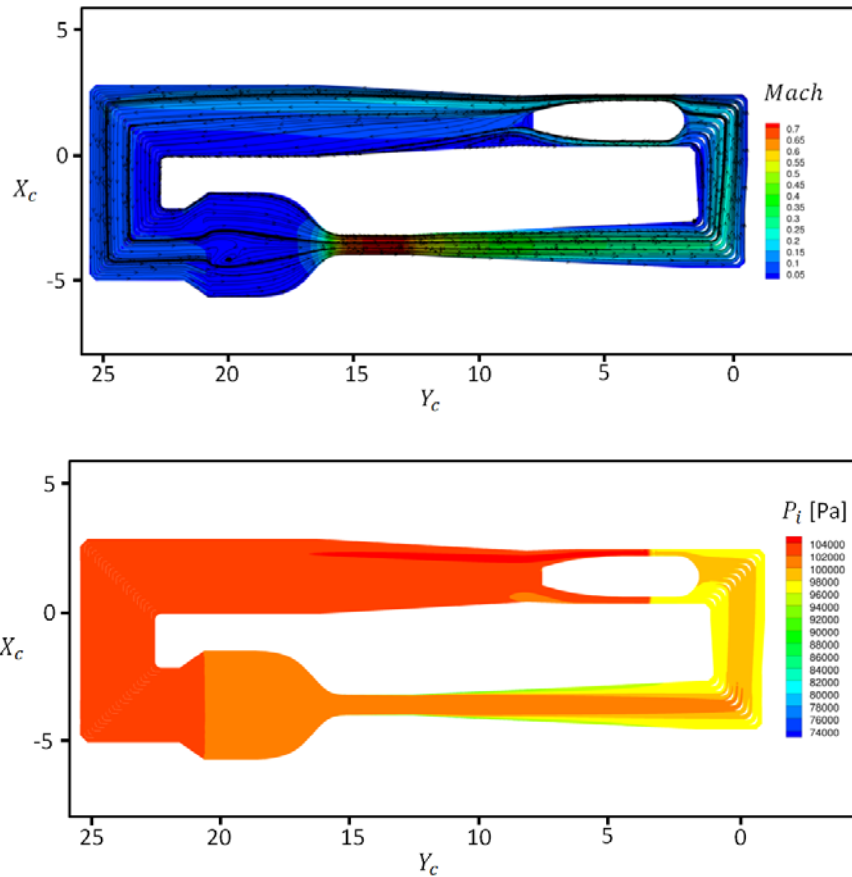


**Figure 2: Result of the RANS simulation for current wind tunnel circuit. The figure shows the flow in a horizontal slice through the circuit at mid-height. (a) Mach number field. (b) Total pressure in Pa.**

The field of total pressure illustrates the effect of the boundary conditions applied at the fan (pressure rise) and the modeling of the heat exchanger (pressure loss).

The realization of the flow in the simulation shows the validity of the set of boundary conditions which allows a converged steady flow solution. In particular one of the difficulty attached to this kind of simulation is the conservation of the mass flow throughout the circuit, which can depends on the meshing strategy (for instance the chimera technique that could have been used to ease the meshing of the vanes is generally not conservative) and the right balance between the heat generated by friction at the walls and the heat exchange at the settling chamber.

The simulated flow shows an overall meaningful behaviour however an asymmetry of the flow downstream of the test section and two zones of separated flow, one downstream of the fan and the other after the wide angle diffuser at the entrance of the settling chamber, are observed. The asymmetry of the flow starts downstream of the test section and grows all the way down to the fan. This results in a side of the fan yielding much faster flow than the other. The velocity difference reduces downstream but only gradually, and it is found to persist down to the wide angle diffuser. The reason for the asymmetry of the flow downstream of the test section is attributed to the natural sensitivity of the flow in a diffuser (here the first diffuser), the asymmetry of the first corner and the absence of fairings in the internal part of corners 1 and 2 in the meshed geometry (although these are present in the real circuit).

## Overview of the recent simulations and experimental works dedicated to the improvement of the ONERA transonic S3Ch wind tunnel

### 3.2 Experimental confrontation

The validation of the numerical simulation against experimental data is uneasy due to the sparsity of the data available along the wind tunnel circuit. While the test section is specifically devoted and designed for measurements, this is not the case of the rest of the circuit. Specific experimental developments would be needed to carry out reasonable comparisons. In the following we carry out comparisons with a reduced set of data in the settling chamber, test section and first diffuser.

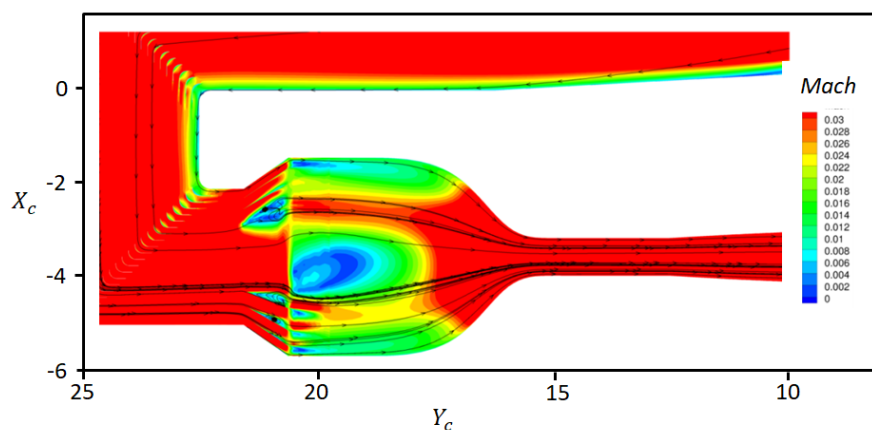


**Figure 3: Close up view of the flow around corners 3 and 4, the rapid diffuser, settling chamber and test section. The Mach number field is shown with a colour map adapted to the low Mach number conditions in the settling chamber. The view is taken on the horizontal plane passing through the centreline of the circuit.**

A close up view of the flow in the region of the last corner of the circuit, again for Mach equal to 0.7 in the test section, is shown in Figure 3. This figure highlights the effect of the vanes of corners 3 and 4 on the flow and that of the cone trunks in the rapid diffuser ahead of the settling chamber. These cone trunks are flow straighteners in the form of thin metal sheets and conical shape about the flow centreline that are inserted inside the rapid diffuser to help guide the flow and cope with the wide angle diffusion. Due to their thinness these cone trunks are only visible through the detached flow at their surface in Figure 3. Flow separation at the surface of the cone trunk was validated experimentally using oil flow visualisation and the irregularity of the flow in the settling chamber could also be qualified experimentally (see Figure 4 (left)) using a mechanical sampling device made of a vertical rake equipped with 20 Pitot tubes movable along the span-wise direction. The experimental data shows a non-uniformity of the flow for Mach equal to 0.7 in the test section, with the right hand side faster than the left hand side and a velocity deficit in the middle of the settling chamber. The increased stream-wise velocity on the sides is also observed in the numerical simulation as well as the velocity deficit in the middle.

**Overview of the recent simulations and experimental works dedicated to the improvement of the ONERA transonic S3Ch wind tunnel**

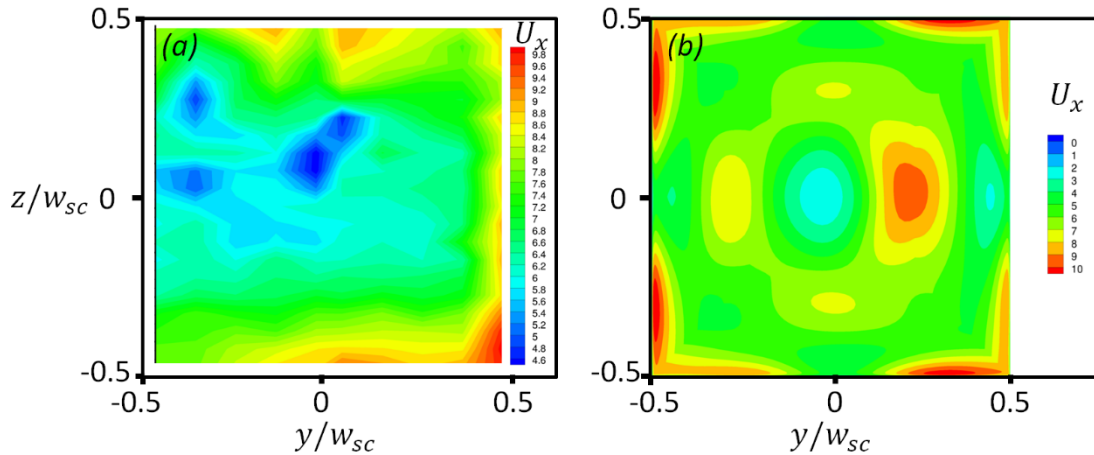


**Figure 4: Axial flow velocity in the settling chamber ahead of the nozzle. (a) The velocity is obtained experimentally using a vertical rake of Pitot tubes placed sequentially at different span-wise location to regularly sample the entire section. (b) The velocity is obtained by the RANS numerical simulation.**

We also confront the simulated data in the test section in terms of the angle formed by the  $v_x$  and  $v_z$  components of the flow velocity against measurements obtained by a clinometer probe traversed vertically at several positions in the span wise direction, see figure 5, that we compare to the numerical results shown in figure 6. The experimental result in figure 5 shows a decrease of the flow incidence  $\alpha = \text{atan}(v_z/v_x)$  in the vertical direction at the mid-span section  $y=0$  and an increase at the side section  $y=15\text{cm}$  while the incidence remains almost uniform at the other side section  $y=-15\text{cm}$ . These variations appear coherent with the numerical findings in Figure 6 with the middle section showing also a decrease of the flow incidence in the vertical direction, the side section in the positive axis showing an increase and finally the negative side section showing a closed to homogeneous incidence.

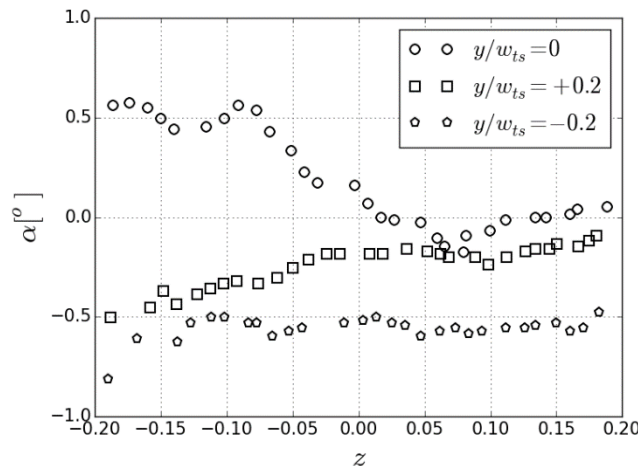


**Figure 5: Angle  $\alpha$  made by the flow velocity components  $v_x$  and  $v_z$  in three different span wise positions, as a function of the vertical coordinate  $z$ , in the test section, for Mach equal to 0.8 in the test section. The results are obtained experimental by a clinometer probe placed on a vertical traverse system.**

**Overview of the recent simulations and experimental works dedicated to the improvement of the ONERA transonic S3Ch wind tunnel**

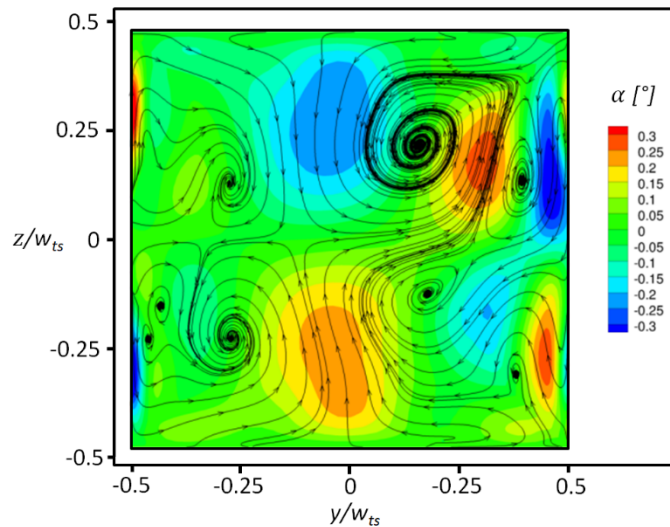


**Figure 6: Flow in the test section obtained from the RANS simulation for Mach 0.7 in the test section. The figure shows a section perpendicular to the circuit axis. The flood iso-contours display the angle  $\alpha$  (in degrees) formed by  $v_x$  and  $v_z$ , the horizontal and vertical velocity components, respectively. The streamlines depicted by the black lines are associated with the  $v_y$  and  $v_z$  components of the flow in the section.**

Figure 7 shows the comparison of stagnation pressure radial profiles at the end of the diffuser between the experiment and the numerical simulation. The pressure loss due to the boundary layer thickening in the diffuser is well predicted.

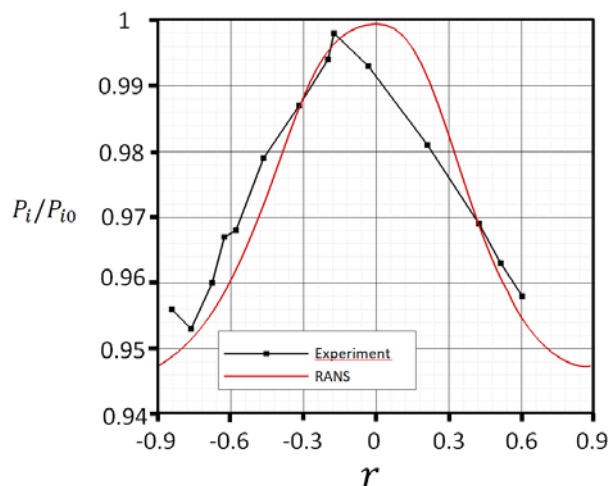


**Figure 7: Comparison of stagnation pressure profiles at the end of the diffuser between experiment in black and numerical simulation in red.**

## Overview of the recent simulations and experimental works dedicated to the improvement of the ONERA transonic S3Ch wind tunnel

### 3.3 New circuit design

A novel design of the S3Ch wind tunnel is proposed based on the previous numerical analysis. Considerations on standard rules of wind tunnel design are also taken from Jaarsma [7], in particular concerning the dimensioning of the turbulence devices (honeycomb, turbulence grids) in the settling chamber. On this topic, it appears that the length of the shape ratio (width to length) of the cells of the honeycomb in the current S3Ch setting is too large and that their width, which should scale on the separation distance between the vanes of the 3<sup>rd</sup> corner, is too small. As a consequence, following these standard rules a shorter honeycomb with wider cells should be integrated in the new design. Jaarsma also provides rules for the grid properties. On this matter, the first turbulent grid should be at an adequate distance from the honeycomb, which is based on the honeycomb cell width. Here the current distance is too large. The properties of a new honeycomb will hence have to be defined following these rules for choosing the right longitudinal distance. In the original S3Ch design, the two grids are identical. The general rule is that the downstream grid should however be thinner. Furthermore the grid porosity is too small compared to the standard value (80%), meaning that the wires of the grid are too thick.

In its general dimensions, the new circuit has been widened by 1 meter to enlarge the operation zone around the test section. This is particularly important for the installation of the optical devices (camera, lasers) whose use has largely increased in the past 20 years. The circuit has also been lengthened by 2 meters, to allow for a longer settling chamber. Another change concerns the vanes of corners 3 and 4 which consisted in curved metal sheets and have been replaced by thick profiles in the new layout. The rapid diffuser upstream of the heat exchanger has been lengthened and the shape of the cone trunks has been modified.

The final design is shown along with the plot of the results of the numerical simulation in Figure 8. Following the previous figures, we display the Mach number field in the horizontal plane at mid-height. Note that the Mach in the test section is now equal to 0.65. The flow defects that were observed in the simulation of the current design are still present, namely the separated flow in the zone around the 1<sup>st</sup> and 2<sup>nd</sup> corners (see at the end of section 3.1 for the discussion on this). Furthermore the flow is also separated in the settling chamber. No further work was accomplished following these results due to the difficulty, already noticed above, to evaluate the validity of the simulation in these areas of separated flows. Albeit the remaining uncertainties about the flow behaviours in these regions, the size increment of the tunnel and particularly that of the settling chamber make us confident about the improvement of the flow. Therefore this design is the one chosen for the future implementation of the tunnel.

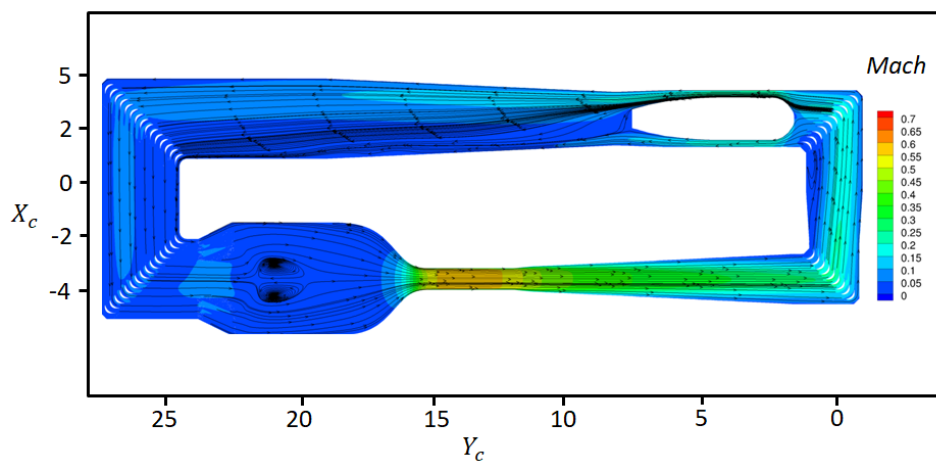


**Figure 8: Field of Mach number in a horizontal section aligned with the circuit centreline for the new design of the S3Ch wind tunnel. The simulated case corresponds to Mach equal to 0.65 in the test section.**

---

## Overview of the recent simulations and experimental works dedicated to the improvement of the ONERA transonic S3Ch wind tunnel

### 4.0 EVALUATION OF A RANS BASED METHOD TO CALCULATE THE SHAPE OF THE ADAPTIVE WALLS

#### 4.1 Analysis of the current method and new opportunities

We described earlier the current method for the calculation of the shape of the adaptive walls, based on the linearized potential flow theory. This representation of the flow inside the test section has many advantages. First the model of the flow is matched with its measured signature, in terms of wall pressure, at the walls. This creates a model which is coherent with the experiment setup. Second the linearity of the effects of the walls and models on the total flow is ideally suited to isolate the effect of the walls and minimize their effects at the exact location of the model. A side output of the method is the corrected Mach number that approaches the Mach number of the flow in free flight, which is the quantity of interest for the numerical analysis when the effects of walls are discarded. Third the method does not require any meshing step, and any case can be easily setup by specifying the right set of singularities to represent the model (and possibly stings or additional bodies present inside the test section). Fourth the tool calculates the ideal shape in a negligible time, which allows its use directly during the wind tunnel tests, without extra preparation.

However the linearized potential flow approach has some limitations. We expect its validity to be questionable when the experimental body is large or when aerodynamic forces are high (especially the lift force). A legitimate question pertains to the effect of shock waves, which can be of a non-negligible size relatively to the test section, especially for two-dimensional bodies (e.g. wing airfoil). The linearized potential flow approach considers a completely smooth flow and no shock. Finally there is also a pragmatic problem related to the maintenance of the tool, which is completely handled by a single person today. Maintaining the skill of this specific tool in this situation is difficult. For all these reasons, the idea to use a more generic and realistic flow solver, like CFD, would be valuable to improve the representation of the flow, remove the linearity condition and spread the skill over a larger number of persons (the CFD code could be used as a black box).

In the following section we detail the developments that were made to evaluate the use of a RANS model of the flow to calculate the shapes of the walls and preliminary results. Our approach is based on an optimization approach in which the shapes of the upper and lower walls are modified so as to reduce the difference between the confined flow and the same flow without wall effect. In particular, we do not follow the standard interface matching approach (see for instance Ganzer [8]) due to the difficulty in accounting for the boundary layers at the walls in this approach.

#### 4.2 Flow model and optimization principle

We are interested in the mean flow and obtain it using a turbulent closure of the averaged Navier-Stokes equations. As before the one equation Spalart-Allmaras turbulent model is used. The calculation of the adaptive walls is carried out by an optimization procedure that targets the minimization of the difference between the two following realizations of the flow of interest:

- Flow **A** in free flight condition
- Flow **B** constrained by the test section

## Overview of the recent simulations and experimental works dedicated to the improvement of the ONERA transonic S3Ch wind tunnel

These two flows are illustrated in Figure 9 in the case of the OALT25 airfoil, an ONERA made laminar transonic airfoil (see also Figure 10 that shows the airfoil installed in the test section). The flow being essentially 2D, a 2D numerical configuration is adopted, meaning that the effect of side walls is not considered in this study. The airfoil chord is  $c$ . The minimization problem writes formally

$$\min_{y_{wall}}(|\mathbf{q}_A - \mathbf{q}_B|^2) \quad (4)$$

where  $\mathbf{q}_{A,B}$  is a vector representing the state of flows A and B and  $y_{wall}$  is a set of altitudes at several locations along the walls that we use to represent their shape. The minimization procedure searches the best  $y_{wall}$  to reduce the difference between A and B in the sense of the functional in (2).

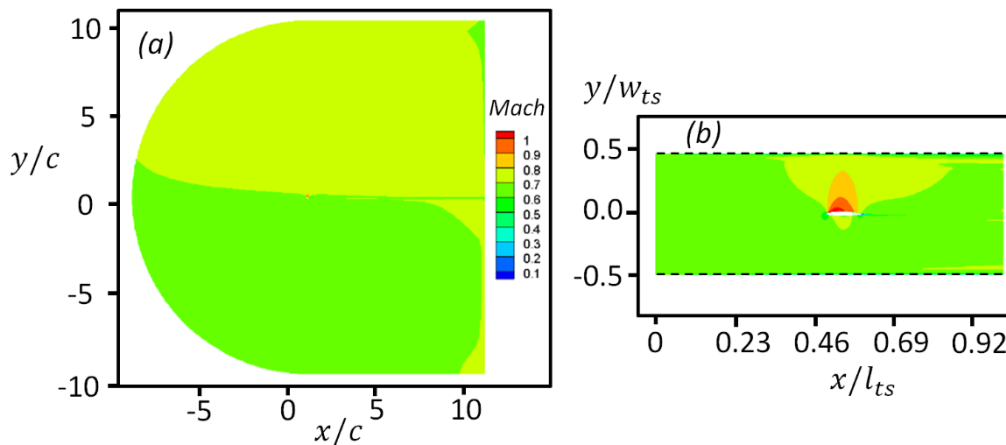


**Figure 9: Illustration of the optimization principle, taking the example of the flow past the OALT25 airfoil in a flow characterized by Mach number equal to 0.7. (a) Flow A in free flight, the external boundary of the domain is set with a freestream type of boundary condition. (b) Flow B inside the test section. The lower and upper boundaries are set with wall type boundary conditions, and the left and right frontiers are set with inflow (total pressure and enthalpy and flow direction) and outflow (static pressure) boundary conditions.**

The complete shape of the wall is determined using a cubic spline interpolation that takes into account a fixed origin and a horizontal tangent of the wall at its upstream end and the nullity of the 2<sup>nd</sup> derivative at the downstream end. In practice we use 3 control points, located in the region of the model for each wall and the optimization problem is solved using the Nelder-Mead algorithm. It was noticed that the use of too many control points can lead to irregular shape of the wall after optimization therefore one need to reduce this number to a low value. The optimization procedure starts from flat walls, then the Nelder-Mead algorithm evaluates the sensitivity of the minimized quantity to variations of the altitude of the control points and the global minimum is found by iterating. At all iteration the mesh is renewed with the given set of position of the control points. The process typically converges in 100 iterations for a reduction of  $O(10^{-3})$  of the target quantity.

## Overview of the recent simulations and experimental works dedicated to the improvement of the ONERA transonic S3Ch wind tunnel



Figure 10: Picture showing the OALT25 airfoil installed in the test section of the S3Ch wind tunnel. View from upstream.

### 4.3 Results

An optimization is carried out with the previous wing airfoil, considering an upstream Mach number equal to 0.75. In this situation, a shock forms at the upper surface of the airfoil. The functional for the optimization is set as  $\sum_{j=1..N} (p_{Aj} - p_{Bj})^2$  that is  $\mathbf{q}_{A,B} = (p_{A,Bj})_{j=1..N}$  is taken as the vector discretizing the complete pressure distribution at the surfaces (upper and lower) of the airfoil in cases A and B in  $N$  discrete values.

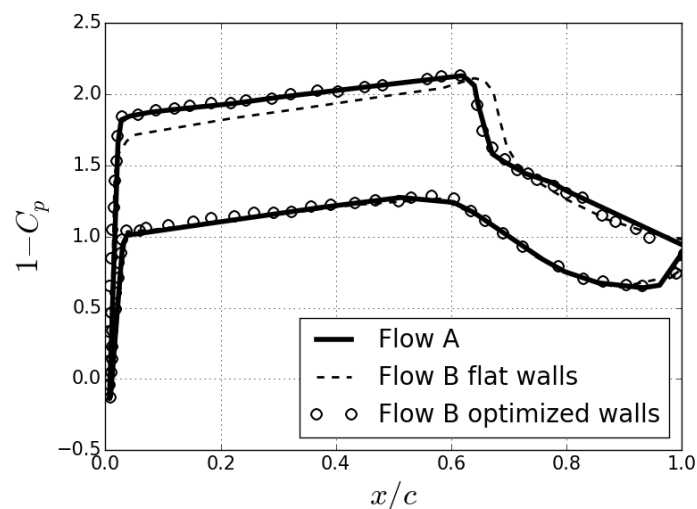


Figure 11: Pressure distribution for the OALT25 airfoil for Mach number equal to 0.75. Three curves are shown. The first one is for flow A in free flight. The second is for flow B with the flat walls and the third one is for flow B with the optimized wall, showing perfect match with flow A. Note that the steep compression is due to the shock wave forming at the upper surface of the wing at this Mach number.

### Overview of the recent simulations and experimental works dedicated to the improvement of the ONERA transonic S3Ch wind tunnel

The optimization output is shown in Figure 11, with pressure distributions around the airfoil. Starting from the flat wall, and a pressure distribution that differs significantly from the free flight configuration (flow A), the optimized walls manage to reproduce exactly the target flow (flow A). The resulting flow field is shown in Figure 12, in terms of Mach number iso-contours and the inset (b) of this figure shows a comparison of the flow iso-contours (again, in terms of Mach number field) between flow A and the optimized flow B. The agreement between the two flows is also obtained; this indicates that matching the pressure distribution allows matching the flow in the vicinity of the body. Lastly Figure 13 shows the optimized deformations of the walls obtained with the current linearized potential flow approach (using the experimental pressure set for the flow past the airfoil) and the present RANS based approach, obtained by the previously described numerical method (which does not account for the pressure measurements at the walls). While the overall trend is well reproduced, there are quantitative differences that are currently under analysis.

Note that other choices were tested for the functional, for instance  $\mathbf{q}=(u_j, v_j)_{j=1..N}$  where  $(u_j, v_j)$  are the flow velocities at a selection of locations around the body. The optimization in this case is not as robust as the previous wall pressure method because there can be discontinuities of the velocity field in transonic flows due to shocks, that the optimization procedure is not able to handle.

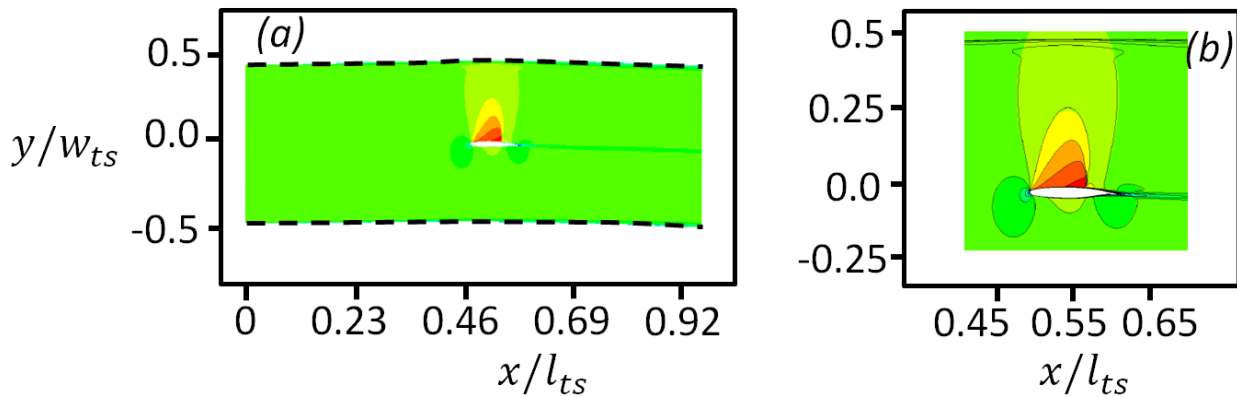
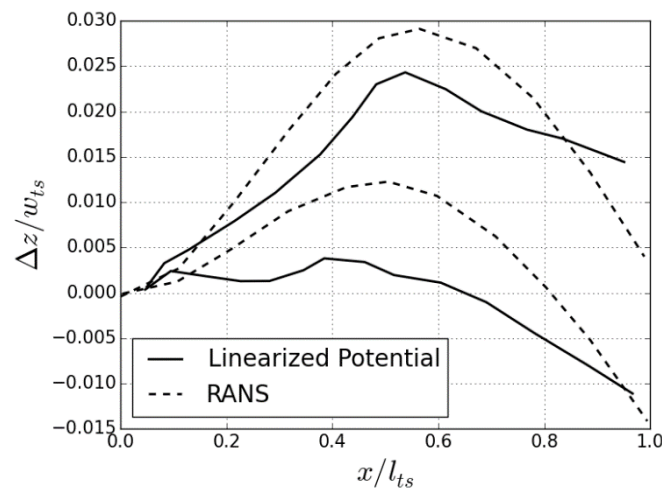


Figure 12: Flow field past the OALT25 airfoil in terms of Mach number (same colormap as Figure 9). (a) View of the complete flow past the airfoil in the test section with the deformed walls calculated by the RANS model. (b) Comparison between flows A and B (see Figure 9 for the references A and B). The flood contours correspond to flow A (free flight), and the lines iso-contours correspond to flow B (with walls).



---

## Overview of the recent simulations and experimental works dedicated to the improvement of the ONERA transonic S3Ch wind tunnel

**Figure 13: Wall deformation  $\Delta z$ , top and bottom, obtained with the current tool based on linearized potential and with the newly developed RANS based optimization tool, for Mach equal to 0.75 in the test section.**

### 5.0 CONCLUSION

In this paper, we present the numerical simulation of the mean flow about the circuit of the S3Ch wind tunnel, as well as comparison against experimental measurements and proposals for a new design of the circuit to improve the quality of the flow. In a second part of the work we describe a new procedure to calculate the shape of the adaptive upper and lower walls of the test section using a RANS model of the flow, instead of the current linearized potential flow approach.

The work is promising for the improved knowledge and control of the flow of the S3Ch wind tunnel. Much needs to be done still concerning the validation of the numerical simulations, since currently only little experimental data is available. In particular, most of it relates to the test section while the validation would require data at a well sampled set of locations all along the circuit. This sets a challenging task for obtaining data at other locations than the test section. Other attempts than those described in the present article to do so were only mildly successful. Certain zones of the wind tunnel of very large dimensions are particularly difficult to handle, and a systematic difficulty is the absence of optical access or nearby acquisition hardware.

The RANS based optimization procedure of the adaptive walls is a first fruitful attempt to change the current methodology. It appears that the definition of the optimization problem is not as straightforward as with the linearized potential flow method, which allows to isolate the effect of the wall and thus, to minimize its effect at any location inside the test section. This is not possible with the CFD approach, and the example that was treated here, the airfoil case, may not generalize easily to more complex geometries. However we proved the possibility to perfectly match the free flight flow for this 2D setting. Further work is needed to see whether this new approach can bring the same ease of use, rapidity and precision as the current method.

### REFERENCES

- [1] Brion, V., Dandois, J., Mayer, R., Reijasse, P., Lutz, T. and Jacquin, L. (2020). Laminar buffet and flow control. *Proc IMechE Part G: J Aerospace Engineering*, Vol. 234(1) 124–139
- [2] L. Jacquin, P. Molton, S. Deck, B. Maury, and D. Soulevant (2009). Experimental study of shock oscillation over a transonic supercritical profile. *AIAA journal*, 47(9):1985{1994}
- [3] Brion, V., Lepage, A., Amosse, Y., Soulevant, D., Senecat, P., Abart, J. C., & Paillart, P. (2015), Generation of vertical gusts in a transonic wind tunnel. *Experiments in Fluids*, 56(7), 1-16
- [4] Torngren, L., Grunnet, J., Nelson, D., and Kamis, D. (1990). The new FFA T1500 transonic wind tunnel initial operation, calibration, and test results. In *16th Aerodynamic Ground Testing Conference* (p. 1420).
- [5] Le Sant, Y. and Bouvier, F. (1992). A new adaptive test section at ONERA Chalais-Meudon, *European Forum on Wind Tunnels and Wind Tunnel Test Techniques*, Southampton University (UK), September 14-17.

---

**Overview of the recent simulations and experimental works dedicated to the improvement of the ONERA transonic S3Ch wind tunnel**

- [6] Cambier, L., Heib, S. and Plot, S. (2013). The Onera elsA CFD software: input from re-search and feedback from industry. *Mechanics & Industry*, EDP Sciences, 14 (3), pp.159-174.
- [7] Jaarsma, F. (1996). General design aspects of low speed wind tunnels, in *Aerodynamics of Wind Tunnel Circuits and their Components*, AGARD CONFERENCE PROCEEDINGS 585.
- [8] Ganzer, U. (1985). A review of adaptive wall wind tunnels. *Progress in Aerospace Sciences*, 22(2), 81-111.

